DEM Generation from MGS NA Stereo Images

Rajagopalan Rengarajan, Jong-SukYoon, Jie Shan*
Geomatics Engineering
School of Civil Engineering
Purdue University
550 Stadium Mall Drive
West Lafayette, IN 47907-2051

1. Introduction

One of the primary tasks of the Mars Global Surveyor (MGS) mission is to produce precision mapping products over the Mars surface [Albee et al, 2001]. Properties and capabilities of MOC NA (Mars Orbiter Camera, Narrow Angle) stereo images for digital elevation model (DEM) generation are studied [Ivanov and Lorre, 2002; Kirk, et al, 2002]. DEM over selected candidate landing sites are produced and their suitability for landing mission is analyzed [Kirk, et al]. However, due to the lack of distinct features and poor contrast of the MOC images, the available commercial photogrammetric tool cannot provide sufficient and reliable matching results for DEM production. This paper presents a solution and evaluates its uncertainty.

2. Image matching

The generation of DEM needs a large number of measurements of corresponding points on the two images of a stereo pair. These measurements are often produced via image matching. In our study, a few steps are involved in this process. First, a number of well-identified points are manually measured in a stereo pair. These measurements are input into a commercial digital photogrammetric tool as 'seed points' to generate more corresponding points. In our study, about two dozens of points are measured manually and over 140 additional points are generated automatically using the commercial tool. The visual check indicates that the correspondence error is at the level of three (3) pixels and no apparent blunder exists. However, due to the poor contrast of the images, such produced corresponding points are not enough in density and quantity for generating the DEM. Additional effort is needed.

As the second step, we developed a matching methodology that automatically generates mass corresponding image points and evaluates their quality. We first use all the corresponding points generated in the first step to establish an approximate relationship between the two images in the stereo pair. In our study, this relationship is described by a bilinear polynomial, whose coefficients are determined by using all the 'seed points' based on the least squares criterion. For any given point on one image, this relationship is used to predict the initial location of the corresponding point on the other image. A window centered at this initial location is then defined as the searching area to refine the initial predicted location. Cross correlation is used for this refinement. The final location is at the place where the correlation coefficient reaches the maximum within the searching window. In our study, the left image is selected as the master image, while the right one as the slave image. A gird of 10- pixel interval on the left image is matched to the right image. The target window on the left image is chosen as 13*13 pixels, while the searching window on the right image is 17*17 pixels. The best location is the one with the maximum correlation coefficient regardless its magnitude. In total, 33,666 (62 in across track and 543 in along track) points are generated for the Eos Chasma stereo pair.

The final step in our matching method is to assess the quality of this process. As an internal check, we exchange the roles of the left and right images. Namely, the matching results on the right image are matched back onto the left image by using the same matching process. The differences between the results obtained from the backward correlation and the original locations on the left image indicate the uncertainty of the matching process. For the Eos Chasma stereo pair, these differences counted in pixels have $m_x = 0.03$ and $\sigma_x = 1.32$ in along track, and $m_y = -0.06$, $\sigma_y = 1.17$ in across track. Figure 1 presents the histograms of the differences obtained through this forward and backward matching evaluation process. It is shown that over 80% of the matched corresponding points are within one (1) pixel matching uncertainty. Only less than 10% points have a matching uncertainty beyond the range of +/- 3 pixels. Figure 1 also indicates that the matching results in the across track direction have about 10% more points within the +/- 1 pixel uncertainty range than the results in the across track direction. The uncertainty distribution follows the Gaussian belt curve.

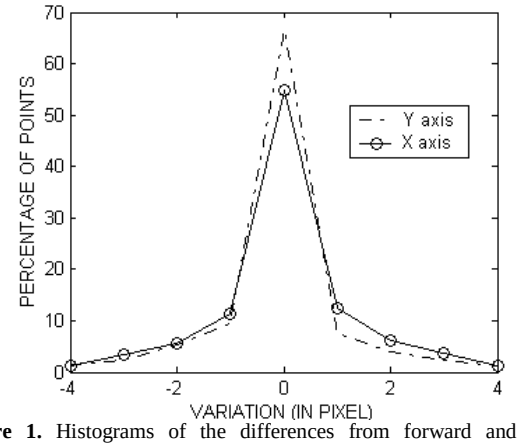

Figure 1. Histograms of the differences from forward and backward matching results (dash: across track; solid: along track; x-axis: pixels; y-axis: number of points in percentage)

Figure 2 plots the histograms of correlation coefficients in the forward and backward matching. It is shown that both process yield almost the same distribution. Due to the poor image contract, about 60% of the total points have a correlation coefficient less than 0.2. Good correlation (correlation coefficient larger than 0.60) can only be reached at about 7% of the total points.

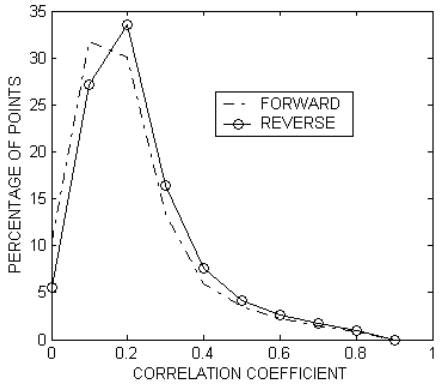

Figure 2. Histograms of correlation coefficients for forward and backward matching (dash: forward; solid: backward, x-axis: correlation coefficient; y-axis: number of points in percentage)

As an external check, the same technique for quality assessment is applied to a total of 162 seed points, whose coordinates are measured manually and by using the commercial photogrammetric tool. The results are plotted in Figure 3.

*corresponding author, can be contacted at jshan@purdue.edu

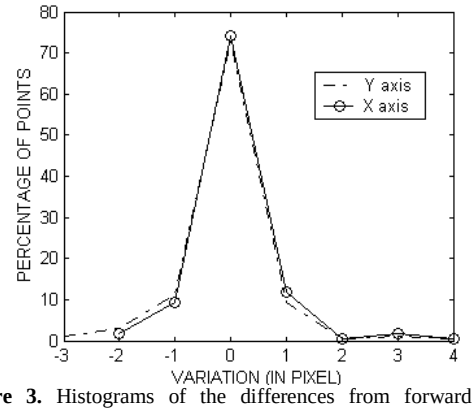

Figure 3. Histograms of the differences from forward and backward matching results (Seed points. dash: across track; solid: along track; x-axis: pixels; y-axis: number of points in percentage)

From the above distribution it is seen that about 95% of the seed points can be re-determined to their original location within the uncertainty of +/- 1 pixel. The overall matching uncertainty in pixels for the entire seed points is $m_x = 0.08$, $\sigma_x = 0.76$ in along track, and $m_y = -0.04$, $\sigma_y = 0.82$ in across track.

Figure 4 plots the histograms of the correlation coefficients for the forward and backward matching of the seed points. It can be seen that over 50% of the seeds points have a correlation coefficients larger than 0.6. This is the best correlation that can be achieved at well-identified points selected either manually or automatically by the feature extraction process in the commercial photogrammetric tool.

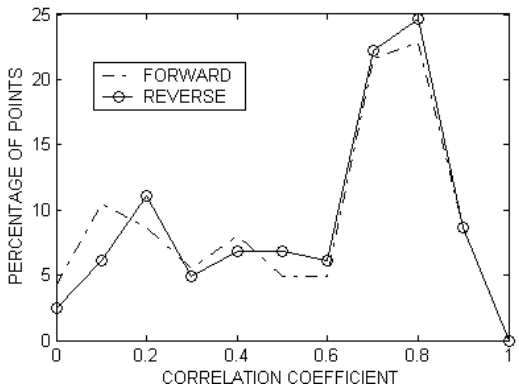

Figure 4. Histograms of correlation coefficients for forward and backward matching (Seed points. dash: forward; solid: backward, x-axis: correlation coefficient; y-axis: number of points in percentage)

3. DEM generation

The DEM is generated using the mass points obtained from automatic matching process. First, we extract the exterior orientation of the two images in a stereo pair from MGS trajectory data [Shan et al, 2002]. Intersection calculation is then performed to determine the 3D coordinates of the matched corresponding points [Shan et al, 2003]. For the Eos Chasma data set, the mean and standard deviation in pixels of the intersection residuals are $m_1 = -21.6$ and $\sigma_1 = 27.6$ on the left image, and $m_2 = 13.1$ and $\sigma_2 = 16.0$ on the right image. All this calculation is performed under the IAU 2000 Cartesian coordinate system, which is then converted to the geographic coordinate and projected for DEM generation. The orthometric heights of the DEM are calculated by correcting the Martian geoid undulation obtained from MOLA archive. DEM at a ground spacing of 20 meters over the Eos Chasma site is produced. Figure 5 presents a 3D view of the DEM.

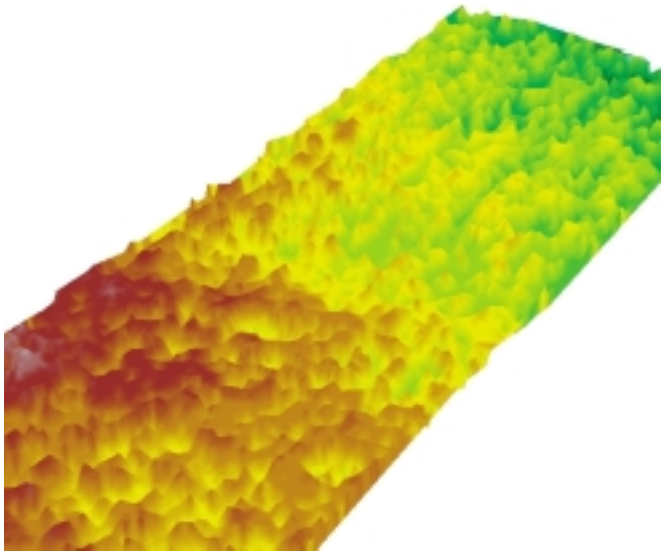

Figure 5. DEM for Eos Chasma area at ground spacing 10m and Z-exaggeration factor 2.

4. Conclusions

The lack of distinct features and poor contrast on Mars surface images cause certain difficulty for commercial tools to generate reliable DEM products. Additional effort is needed to achieve reliable image matching and understand its quality. Future work will be focused on image matching with sub-pixel accuracy and higher reliability, and precision sensor modeling to further improve the DEM quality.

5. References

[1] Albee, A. L., Arvidson, R. E., Palluconi, F., Thorpe, T., 2001. Overview of the Mars Global Surveyor mission, Journal of Geophysical Research, Vol. 106, No. E10, October 25, pp. 23,291-23,316.

[2] Ivanov, A.B., Lorre, J.J., 2002. ANALYSIS OF MARS ORBITER CAMERA STEREO PAIRS, The 33rd Lunar and Planetary Science Conference, March 11–15, League City, TX.

[3] Kirk, R. L., Soderblom, L. A., Howington-Kraus, E., Archinal, B., 2002. High resolution topomapping of Mars with Mars Orbiter Camera Narrow-angle Images, IAPRS, Vol.34, Part 4, "GeoSpatial Theory,Processing and Applications", Ottawa, CD-ROM.

[4] Shan, J., Lee, D.S., Yoon, J-S., 2002. Photogrammetric Registration of MOC imagery with MOLA data, Joint International Symposium on Geospatial Theory, Processing and Applications Ottawa, Canada, 8-12 July, on CD-ROM.

[5] Shan, J., Yoon, J-S., Lee, D.S., et al, 2003, Photogrammetric Reduction of Mars Global Surveyor Data, submitted to Photogrammetric Engineering and Remote Sensing.